UC Santa Barbara
UC Santa Barbara Previously Published Works

Title

Atlantic overturning responses to obliquity and precession over the last 3 Myr

Atlantic overturning responses to obliquity and precession over the last 3 Myr

L. E. Lisiecki[1]

[1] Department of Earth Science, University of California, Santa Barbara, California, USA

Abstract This study analyzes 39 Atlantic and seven Pacific benthic δ^{13}C records to characterize obliquity and precession responses in Atlantic overturning since 3 Ma. Regional benthic δ^{13}C stacks are also analyzed. A major transition in orbital responses is observed at 1.5–1.6 Ma coincident with the first glacial shoaling of Northern Component Water. Since ~1.5 Ma, the phases of Atlantic benthic δ^{13}C records from 2300 to 4000 m depth lag maximum obliquity by 59° (6.7 kyr) and June perihelion precession forcing by 133° (8.5 kyr). Comparison with North Atlantic sea surface temperature suggests that these orbital responses (particularly precession) in middle deep Atlantic δ^{13}C are associated with changes in ocean heat transport and overturning rates. The mid-Pleistocene transition had little effect on the obliquity and precession phases of benthic δ^{13}C but did result in a ~50% decrease in the obliquity power of middle deep Atlantic δ^{13}C at 0.6 Ma.

1. Introduction

Changes in ocean circulation are thought to play an important role in both orbital and millennial climate change throughout the Pleistocene [*Imbrie et al.*, 1992; *McManus et al.*, 2004; *Raymo et al.*, 1998; *Bartoli et al.*, 2006], but the causes of orbital-scale circulation change in particular are not well understood. Most previous studies have either evaluated orbital-scale circulation responses by analyzing benthic δ^{13}C gradients between strategically selected sites [e.g., *Oppo and Fairbanks*, 1987; *Flower et al.*, 2000; *Hodell and Venz-Curtis*, 2006] or by reconstructing "snapshots" of spatial variability using δ^{13}C from many sites at particular times [e.g., *Curry and Oppo*, 2005; *Raymo et al.*, 2004; *Hesse et al.*, 2011]. *Lisiecki et al.* [2008] developed a complementary approach in which the phases of orbital responses at many sites were analyzed to identify both the timing and spatial extent of Atlantic circulation changes. By comparing the obliquity and precession phases of Atlantic benthic δ^{13}C from 0 to 0.4 Ma, *Lisiecki et al.* [2008] found that changes in Northern Component Water (NCW) formation were not consistently explained by forcing from either Northern Hemisphere (NH) summer insolation (i.e., Milankovitch forcing) or ice sheet size. However, they were unable to distinguish between a variety of alternative forcing mechanisms.

In this study the methodology of *Lisiecki et al.* [2008] is extended to benthic δ^{13}C throughout the last 3 Myr. Both this study and *Lisiecki et al.* [2008] focus on the phases of obliquity and precession responses in an attempt to reconstruct the causal sequence of climate responses associated with these cycles. Obliquity and precession responses differ fundamentally from 100 kyr glacial cyclicity because local, seasonal insolation provides strong obliquity and precession forcing but contains negligible 100 kyr power. Therefore, obliquity and precession responses can be directly compared to proposed insolation forcing, whereas the cause of 100 kyr cyclicity is uncertain and often attributed to complex feedback within the climate system [e.g., *Bintanja and van de Wal*, 2008; *Lisiecki*, 2010a; *Rial et al.*, 2013; *Abe-Ouchi et al.*, 2013]. Establishing a better understanding of how the climate system responds to known obliquity and precession forcing should aid the interpretation of 100 kyr climate responses.

2. Background

2.1. Orbital Changes in Atlantic Overturning

Today NCW fills most of the deep Atlantic from 2000 to 4000 m, but during late Pleistocene glaciations NCW shoaled to above about 2000 m and was replaced at depth by Southern Component Water (SCW) [e.g., *Curry and Oppo*, 2005; *Hesse et al.*, 2011]. This shift may have been caused by large changes in the densities of NCW and SCW [*Miller et al.*, 2012] and was likely crucial for sequestering CO_2 in the deep ocean during glacial maxima [e.g., *Sigman et al.*, 2010]. However, it is unclear how glacial overturning rates compared to modern and whether changes in NCW were primarily driven by northern or southern forcing [e.g., *Shin et al.*, 2003;

Lisiecki et al., 2008]. Ocean models differ in their estimations of which mechanisms are most important and what kinds of NCW change are predicted [*Weber et al.*, 2007].

Early work suggested that changes in Atlantic overturning were likely driven by changes in ice volume because benthic δ^{13}C record from Deep Sea Drilling Project (DSDP) Site 607 at 3400 m in the North Atlantic slightly lagged ice volume in both the obliquity and precession bands [*Imbrie et al.*, 1992]. However, other analyses have revealed significant differences in obliquity and precession phases of δ^{13}C relative to ice volume, particularly along the deep western boundary current [*Curry*, 1996; *Bickert et al.*, 1997; *Flower et al.*, 2000; *Lisiecki et al.*, 2008; *Hodell et al.*, 2013]. Additionally, the phases of sea surface temperature (SST) in the North and tropical Atlantic suggest that these benthic δ^{13}C responses are accompanied by changes in northward heat transport and hence overturning rate [*Lisiecki et al.*, 2008]. Because Atlantic overturning responded differently to obliquity and precession forcing, circulation changes since 0.4 Ma cannot be explained solely as responses to NH summer insolation or ice volume. *Lisiecki et al.* [2008] highlighted two possible insolation forcings that are consistent with the observed orbital phases, high-latitude southern summer insolation and high-latitude northern September insolation, but neither could be definitively linked with overturning.

2.2. Pleistocene Transitions in Circulation

Many studies suggest significant changes in Atlantic circulation between 1.8 and 1.5 Ma. Increases in %NCW in the deep equatorial Atlantic unaccompanied by increases in %NCW at shallower sites suggest that the NCW-SCW boundary deepened at ~1.8 Ma [*Venz and Hodell*, 2002]. Additionally, δ^{13}C gradients indicate that glacial shoaling of NCW began or increased greatly at ~1.6 Ma [*Bickert et al.*, 1997; *McIntyre et al.*, 1999]. A concurrent reduction in the benthic δ^{13}C of the deep South Atlantic relative to the deep Pacific argues for a corresponding decrease in the ventilation of deep SCW [*Venz and Hodell*, 2002; *Hodell and Venz-Curtis*, 2006].

During the mid-Pleistocene transition (MPT) at ~0.8 Ma, benthic δ^{13}C records show a large increase in 100 kyr power and further intensification of NCW glacial shoaling [*Raymo et al.*, 1997]. North Atlantic cooling also occurs throughout the MPT as recorded by SST and bottom water temperature at Site 607 (and redrilled as Integrated Ocean Drilling Program (IODP) Site U1313) [*Ruddiman et al.*, 1989; *Sosdian and Rosenthal*, 2009; *Lawrence et al.*, 2010; *Naafs et al.*, 2012]. After the MPT (~0.6 Ma), an increase in the interglacial δ^{13}C value of NCW originating from the Norwegian-Greenland Sea likely indicates a reduction in sea ice due to "extreme interglaciation" [*Raymo et al.*, 2004].

2.3. Benthic δ^{13}C as a Proxy for NCW

The δ^{13}C of carbonate from benthic foraminifera is often used to estimate past changes in the spatial extent of NCW. The δ^{13}C of dissolved inorganic carbon (DIC) is initially set by surface water processes at the time of deep water formation and then altered by the gradual accumulation of remineralized low-δ^{13}C organic carbon in the deep ocean, sometimes described as an "aging" effect [e.g., *Curry et al.*, 1988]. Additionally, the mean δ^{13}C of the whole ocean varies by 0.32–0.46 ‰ as the result of glacial changes in terrestrial carbon storage [*Duplessy et al.*, 1988; *Curry et al.*, 1988; *Tagliabue et al.*, 2009].

Due to the relatively short residence time of deep water in the Atlantic, Atlantic benthic δ^{13}C records are generally considered to reflect changes in the δ^{13}C values of NCW and SCW and their mixing ratios at each site [e.g., *Oppo and Fairbanks*, 1987; *Flower et al.*, 2000]. Modern North Atlantic Deep Water is characterized by a more positive DIC δ^{13}C value (~1‰) than Antarctic Bottom Water (~0.2‰) [*Kroopnick*, 1985]. An even larger difference in the benthic δ^{13}C values is observed during Pleistocene glacial maxima (e.g., 1.5‰ for NCW and −0.5‰ for deep SCW during the Last Glacial Maximum [*Curry and Oppo*, 2005; *Hesse et al.*, 2011]). However, there is evidence that before 0.6 Ma NCW from the Norwegian-Greenland Sea had substantially lower δ^{13}C values, i.e., ~ 0.2‰ at Ocean Drilling Program (ODP) Site 984 [*Raymo et al.*, 2004].

Although glacial decreases in deep Atlantic δ^{13}C are generally interpreted as decreases in %NCW caused by NCW shoaling and the northward incursion deep SCW [e.g., *Oppo and Fairbanks*, 1987; *Curry and Oppo*, 2005; *Hesse et al.*, 2011], some studies suggest that deep Atlantic δ^{13}C records may be more indicative of changes in SCW ventilation than large-scale NCW shoaling [*Piotrowski et al.*, 2005; *Gebbie*, 2014]. Additionally, there is evidence for nonconservative changes in Atlantic δ^{13}C at ~2000 m during Heinrich Stadial 1 [*Tessin and Lund*, 2013]. Given these uncertainties, it is difficult to confidently attribute δ^{13}C changes to a specific physical change in circulation (e.g., quantifying %NCW at a particular location). Nonetheless, benthic δ^{13}C records are

still likely indicative of large-scale changes in the ventilation of the deep Atlantic with potentially significant climate impacts, e.g., through changes in ocean carbon storage.

Because benthic δ^{13}C cannot be used as a proxy for overturning rate, this study uses North Atlantic SST records to test for a link between benthic δ^{13}C and overturning rate. Changes in overturning rate should affect northward heat transport and North Atlantic SST. For example, during Heinrich events, reduced overturning is associated with minima in North Atlantic SST [e.g., *McManus et al.*, 2004]. *Lisiecki et al.* [2008] observed that North Atlantic summer SST covaries with middle deep Atlantic δ^{13}C (2300–4010 m) during obliquity and precession cycles of the last 425 kyr. Because North Atlantic SST maxima have the same phase as middle deep Atlantic δ^{13}C maxima but are antiphased with precession maxima in local summer insolation, the most plausible explanation is that North Atlantic SST and δ^{13}C were both affected by changes in overturning rate.

Note that the Atlantic depth range of 2300–4010 m, which *Lisiecki et al.* [2008] called "middepth," is called the middle deep Atlantic in this study to avoid confusion with intermediate-depth water (which here refers to 1000–2300 m). Additionally, Atlantic water below 4010 m (formerly the "deep" Atlantic) is here called the lower deep Atlantic.

3. Methods

3.1. Overview

This study analyzes as many long (>300 kyr) benthic δ^{13}C records as could be obtained from the scientific literature to characterize patterns of orbital-scale circulation change. Most of this study focuses on results from 0 to 1.6 Ma due to the larger number of records, better signal-to-noise ratio, and better phase agreement among middle deep Atlantic δ^{13}C records since 1.6 Ma.

After δ^{13}C records are placed on a common age model (section 3.2), they are analyzed in two ways. First, spectral analysis is performed on individual records to characterize spatial patterns in the phase, amplitude, and coherency of obliquity and precession response. This allows for identification of large-scale patterns (used to define "regions" within the Atlantic) as well as potential outliers. Second, regional δ^{13}C stacks are constructed using long, high-resolution benthic δ^{13}C records from each region. Stacking enhances the signal-to-noise ratio of the δ^{13}C records and reduces potential local effects. Therefore, these regional stacks are particularly useful for identifying transitions in circulation and comparing circulation responses with other climate records.

Links between circulation and other climate responses, such as ice volume and SST, are evaluated by comparing the phases and amplitude modulations of the signals. Phases and amplitudes which covary through time suggest either a causal relationship between signals or potentially independent responses to the same forcing.

3.2. Benthic δ^{13}C Records

This study analyzes previously published benthic δ^{13}C records from 39 Atlantic sites from 1145 to 4620 m depth and seven Pacific sites from 2770 to 3850 m (Table 1 and Figure 1). All of these records are derived primarily from *Cibicidoides* species, which most studies find accurately records the δ^{13}C of deep water DIC [e.g., *Belanger et al.*, 1981; *Graham et al.*, 1981] except in areas of very high productivity [*Mackensen et al.*, 1993]. In a few records the original authors have used other species with species-dependent δ^{13}C corrections during small gaps in the availability of *Cibicidoides* [e.g., *Alonso-Garcia et al.*, 2011].

The age model for each δ^{13}C record (Figure 2) is produced by aligning the core's benthic δ^{18}O record to the LR04 benthic δ^{18}O stack [*Lisiecki and Raymo*, 2005] using an automated algorithm [*Lisiecki and Lisiecki*, 2002]. Benthic δ^{18}O is sensitive to changes in global ice volume, deep water temperature, and local variations in the δ^{18}O of sea water and is often assumed to exhibit globally synchronous variations. Benthic δ^{18}O alignments have uncertainties ± 2 to ± 8 kyr, depending on the temporal resolution of the data and assuming synchronous δ^{18}O responses (L. Lin, personal communication, 2013). However, Pacific δ^{18}O may briefly lag Atlantic δ^{18}O by as much as 4 kyr during terminations [*Skinner and Shackleton*, 2005; *Lisiecki and Raymo*, 2009]. Portions of records with an original resolution of less than one point per 10 kyr are not used for stacking or phase analysis (dotted lines in Figure 2). Additionally, precession phase is only calculated for records with a resolution of at least one point per 5.6 kyr.

Table 1. Core Locations[a]

Site	Latitude	Longitude	Depth (m)	In Stack?	Reference
			Intermediate North Atlantic		
ODP982	57.5	−15.9	1145	Y	*Venz et al.* [1999]
ODP984	61.0	−24.0	1650		*Raymo et al.* [2004]
DSDP502	11.5	−79.4	1800(sill)		*deMenocal et al.* [1992]
ODP983	60.4	−23.6	1983	Y	*McIntyre et al.* [1999]
ODP1088	−41.1	13.6	2083		*Hodell et al.* [2003]
ODP980/981	55.5	−14.7	2169	Y	*Oppo et al.* [1998]; *McManus et al.* [1999]; *Flower et al.* [2000]; *Raymo et al.* [2004]
ODP658	20.8	−18.7	2264	Y	*Tiedemann et al.* [1994]
DSDP552	56.0	−23.2	2301		*Shackleton and Hall* [1984]
			Middle Deep Atlantic		
GeoB1113	−5.7	−11.0	2374		*Sarnthein et al.* [1994]
MD96-2080	−36.3	19.5	2488		*Rau et al.* [2002]
GeoB1032	−22.9	6.0	2500		*Bickert and Wefer* [1996]
U1314	58.4	−27.9	2820		*Alonso-Garcia et al.* [2011]
GIK13519-1	5.7	−19.9	2862		*Sarnthein et al.* [1984]
ODP925	4.2	−43.5	3040	Y	*Bickert et al.* [1997]
ODP659	18.0	−21.0	3071	Y	*Tiedemann et al.* [1994]
GeoB1214	−24.7	7.2	3215		*Bickert and Wefer* [1996]
GeoB1105	−1.7	−12.4	3230		*Bickert and Wefer* [1996]
EW9209-3JPC	5.3	−44.3	3288		*Curry et al.* [1999]
ODP927	5.5	−44.5	3326	Y	*Bickert et al.* [1997]
DSDP607	41.0	−33.0	3427	Y	*Raymo et al.* [1989]; *Ruddiman et al.* [1989]
GeoB1312	−31.7	−29.7	3436		*Hale and Pflaumann* [1999]
EW9209-2JPC	5.6	−44.5	3528		*Curry et al.* [1999]
ODP926	3.7	−42.9	3598	Y	*Lisiecki et al.* [2008]
GeoB1034	−21.7	5.4	3731		*Bickert and Wefer* [1996]
TN0576	−42.9	8.9	3751		*Hodell et al.* [2000]
ODP664	0.1	−23.2	3806	Y	*Raymo et al.* [1997]
U1308	49.9	−24.2	3883	Y	*Hodell et al.* [2008]
GeoB1117	−3.8	−14.9	3980		*Bickert and Wefer* [1996]
ODP928	5.5	−44.8	4010	Y	*Lisiecki et al.* [2008]
			Lower Deep Atlantic		
ODP1090	−42.9	8.9	3702	Y	*Venz and Hodell* [2002]
GeoB1041	−3.5	−7.6	4035		*Bickert and Wefer* [1996]
EW9209-1JPC	5.9	−44.2	4056		*Curry and Oppo* [1997]
GeoB1211	−24.5	7.5	4085	Y	*Bickert and Wefer* [1996]
RC13-229	−25.5	11.3	4191	Y	*Oppo et al.* [1990]
ODP929	6.0	−43.7	4369	Y	*Bickert et al.* [1997]
GeoB1035	−21.6	5.0	4450		*Bickert and Wefer* [1996]
GeoB1101	1.7	−11.0	4570		*Bickert and Wefer* [1996]
ODP1089	−47.9	9.9	4621	Y	*Hodell et al.* [2001]
			Deep Pacific		
ODP846	−3.1	−90.8	3307	Y	*Mix et al.* [1995a]
ODP1208	36.1	158.5	3346	Y	*Venti and Billups* [2012]
ODP677	4.2	−83.7	3461	Y	*Shackleton et al.* [1990]
ODP849	0.2	−110.5	3851	Y	*Mix et al.* [1995b]
ODP1123	−41.8	−171.5	3290	Y	*Harris* [2002]
RC13-110	−0.1	−95.7	3231	Y	*Imbrie et al.* [1992]
ODP1143	9.4	−246.7	2772	Y	*Cheng et al.* [2004]

[a]Y = yes.

3.3. δ^{13}C Versus $\Delta\delta^{13}$C

Previous studies have converted Atlantic benthic δ^{13}C records to %NCW or $\Delta\delta^{13}$C in an attempt to remove responses unrelated to circulation change from the δ^{13}C signals. However, I choose to analyze untransformed δ^{13}C records because performing these transformations requires data that are not well constrained.

If δ^{13}C values for NCW and SCW were known, benthic δ^{13}C records could be converted into changes in %NCW [*Oppo and Fairbanks*, 1987] at core sites throughout the Atlantic. However, estimating the δ^{13}C values of the NCW and SCW mixing end-members through time is quite difficult, particularly because the core sites used to estimate SCW δ^{13}C contain a nonneglible fraction of NCW. For example, ODP Site 1090 at 3700 m in the South Atlantic contains 40% NCW today [*Venz and Hodell*, 2002]. NCW δ^{13}C is also not well
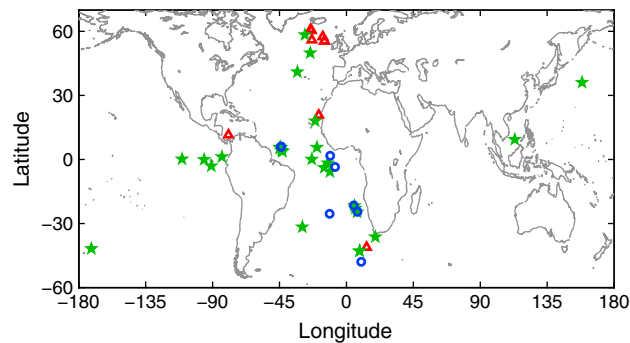
Figure 1. Map of core locations. Symbols denote core depth in meters below sea level: 1000–2301 m (red triangles), 2302–4010 m (green stars), and 4011–4650 m (blue circles).

constrained through time because depleted δ^{13}C values are observed in some intermediate North Atlantic records [*Flower et al.*, 2000; *Raymo et al.*, 2004].

An alternative metric is $\Delta\delta^{13}$C which seeks to remove the signal of mean ocean δ^{13}C change by taking the gradient between Atlantic δ^{13}C records and mean ocean δ^{13}C as estimated from deep Pacific δ^{13}C records [e.g., *Hodell and Venz-Curtis*, 2006; *Lisiecki et al.*, 2008]. There are three reasons why I chose to analyze δ^{13}C rather than $\Delta\delta^{13}$C for this study. (1) Analysis of untransformed δ^{13}C avoids the assumption that mean ocean δ^{13}C is well approximated by the deep Pacific, which represents only ~25% of total ocean volume. (2) The overall results for middle deep Atlantic δ^{13}C and $\Delta\delta^{13}$C are quite similar because orbital responses in Pacific δ^{13}C are relatively weak. (3) Changes in Pacific δ^{13}C response create small systematic shifts in all $\Delta\delta^{13}$C records. By analyzing Atlantic and Pacific δ^{13}C separately, it is easier to identify the source of each change in δ^{13}C.

3.4. Spectral Analysis

The spectral density and phase of each proxy record was calculated using the Blackman-Tukey technique as implemented by the Arand software package (P. Howell, N. Pisias, J. Ballance, J. Baughman, and L. Ochs, Brown University). Before spectral analysis all data were interpolated to an even 1 kyr spacing. Two types
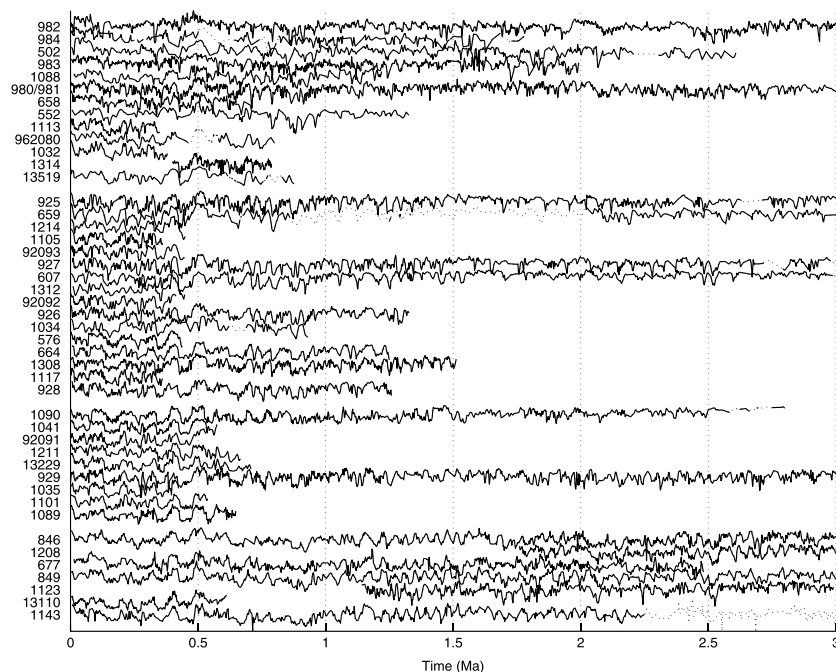
Figure 2. Benthic δ^{13}C records used in this study after sampling at 2 kyr resolution. See Table 1 for citations. Dotted lines indicate portions of records that were excluded from analysis due to sample spacing of >10 kyr.
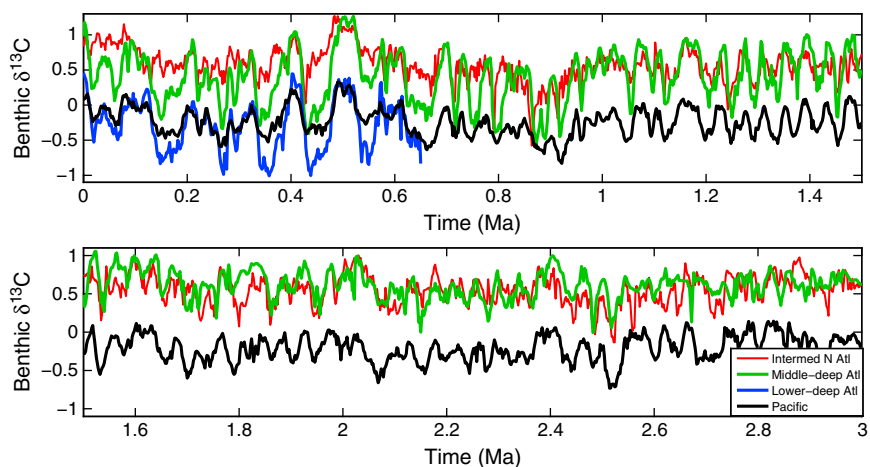
Figure 3. Regional δ^{13}C stacks for the intermediate-depth North Atlantic (red), middle deep Atlantic (green), lower deep Atlantic (blue), and Pacific (black). See Table 1 for a list of cores included in each stack.

of analysis were performed: (1) a moving 400 kyr boxcar window to evaluate changes in the amplitude and phase of obliquity and precession through time and (2) spectral power and phase calculations for 0–1.5 Ma to characterize late Pleistocene orbital responses. The maximum lag for the Blackman-Tukey calculations was set to 50% of the window length. Obliquity and precession responses were calculated at frequencies of 1/40.8 and 1/23 kyr^{-1} with bandwidths of 0.0018 kyr^{-1} for 1.5 Myr windows and 0.0067 kyr^{-1} for 400 kyr windows.

All phase and coherence results are calculated relative to ETP (defined as normalized eccentricity plus normalized obliquity minus normalized precession); therefore, precession phases are reported relative to June perihelion, not maximum precession. Ice volume response is estimated using the LR04 global benthic δ^{18}O stack [*Lisiecki and Raymo*, 2005]; however, changes in deep water temperature could shift the phase of benthic δ^{18}O relative to ice volume [e.g., *Hodell et al.*, 2013]. Phases are shown for negative δ^{18}O and, therefore, represent the phase of minimum ice volume. The absolute phases of δ^{13}C and other climate variables in this study are all dependent upon the LR04 benthic δ^{18}O age model, which has approximately constant obliquity and precession phases from 0 to 1.6 Ma [*Lisiecki and Raymo*, 2005]. Any error in the stack age model would shift the phases of all climate responses by approximately the same amount relative to ETP.

3.5. Benthic δ^{13}C Regional Stacks
Benthic δ^{13}C records from individual sites are used to construct regional δ^{13}C stacks (Figure 3) of the intermediate North Atlantic (1100–2200 m), middle deep Atlantic (3000–4025 m), lower deep Atlantic (4050–4650 m), and deep Pacific (2770–3850 m). Atlantic depth ranges were selected based on distinct patterns of obliquity and precession phases in δ^{13}C records (see section 4.2). However, these stacks should not be interpreted as representing the δ^{13}C values of specific water masses because different amounts of mixing across these boundaries occur through time.

Table 1 shows which cores are included in each stack. Note that the lower deep Atlantic stack includes ODP Site 1090, which is in the middle deep Atlantic (3702 m) but has δ^{13}C values similar to lower deep Atlantic sites due to its southern latitude (42.9°S). Additionally, the lower deep Atlantic stack spans only 0–0.65 Ma because only two of its component record extend beyond 0.65 Ma (Figures 2 and Figure S1 in the supporting information). Before stacking, all benthic δ^{13}C records were converted to have an even 2 kyr sample spacing by linear interpolation or, for data with ≤0.5 kyr spacing, by averaging all data within ±1 kyr. Portions of individual records with an average sample spacing >10 kyr were excluded from the stacks.

Because the mean and amplitude of δ^{13}C records within each region differ slightly depending on a core's precise location, records beginning and ending at different times within a stack could create the false impression of a trend or transition in regional δ^{13}C. To minimize this effect, individual Atlantic records were normalized based on their mean and standard deviation over a 0–0.5 Ma time window before stacking. Then each regional stack was scaled to match the average mean and standard deviation of its component records within that time window. Scaling records based on this relatively short time window allows the Atlantic
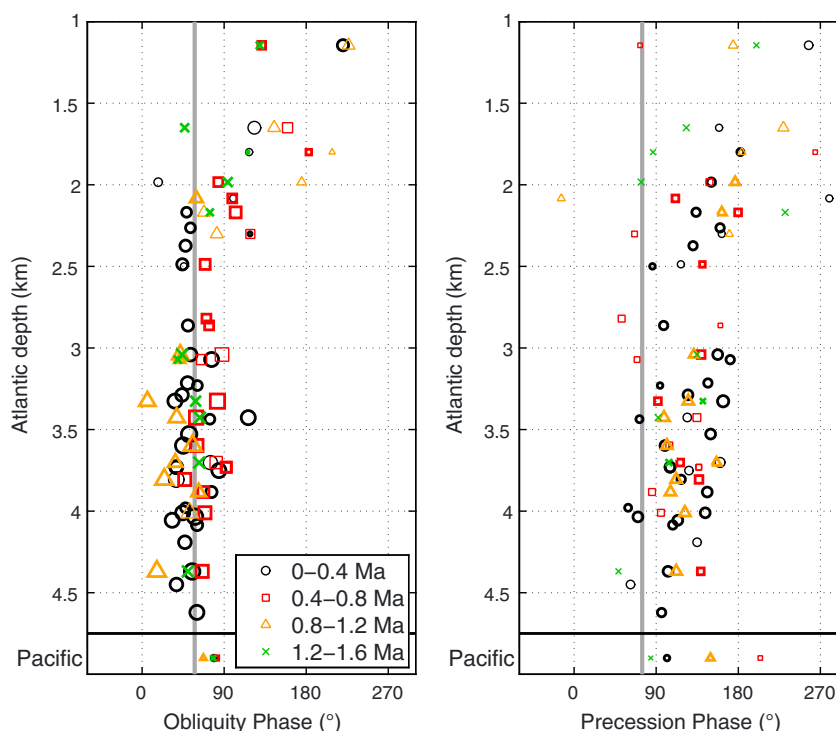
Figure 4. Obliquity and precession phase lags of Atlantic benthic δ^{13}C as a function of depth for 0–1.6 Ma. Pacific δ^{13}C stack phases are shown at the bottom for comparison. Phases are plotted relative to ETP in nonoverlapping 400 kyr windows: 0–0.4 Ma (black circles), 0.4–0.8 Ma (red squares), 0.8–1.2 Ma (orange triangles), and 1.2–1.6 Ma (green crosses). Symbol sizes are proportional to the log of spectral density, and bold symbols indicate 80% coherence with ETP. Vertical gray lines show the mean phase of benthic δ^{18}O from 0 to 1.6 Ma.

stacks to accurately reflect changes in the mean or variance of regional δ^{13}C through time. However, Pacific records were scaled over their entire length because late Pleistocene δ^{13}C data were not available for two of the six stacked Pacific records.

3.6. North Atlantic SST

North Atlantic SST records are used to test for changes in NCW overturning rate. Three long North Atlantic SST records are available from Site 607/U1313 (Figure S2). Summer SST at Site 607 is estimated using foraminiferal species counts from 0 to 1.7 Ma [*Ruddiman et al.*, 1989]. Annual mean SST at Site 607 is estimated using the alkenone unsaturation index ($U^{k\prime}_{37}$) from 0.25 to 3 Ma [*Lawrence et al.*, 2010]. The age model used for both 607 SST records is based on a revised alignment of the site's benthic δ^{18}O to the LR04 stack, which improves obliquity coherence and does not significantly alter SST phases. However, age model uncertainty for this site is ~30 kyr from 0.45 to 0.6 Ma and at ~1.8 Ma due to low-resolution δ^{18}O data.

Mean annual SST from $U^{k\prime}_{37}$ at IODP Site U1313 is also available from 0 to 3 Ma [*Naafs et al.*, 2012]. Because a continuous benthic δ^{18}O record is not available for this core, the U1313 SST record is analyzed using its published timescale [*Naafs et al.*, 2011, 2012] that combines alignment of both high-resolution benthic δ^{18}O (from 0.3–0.7 Ma to 0.8–0.9 Ma) and core lightness to the LR04 benthic stack. Therefore, the U1313 age model and its SST phase estimates are most reliable from 0.3 to 0.9 Ma; uncertainty is greater outside of this interval because phase lags of several kiloyears are observed between benthic δ^{18}O and core lightness in some portions of the core [*Naafs et al.*, 2011, 2012].

4. Results

4.1. Regional δ^{13}C Gradients

Regional δ^{13}C stacks give an overview of Atlantic circulation responses over the past 3 Myr and show many of the same features observed in previous studies (Figure 3). The gradient between the intermediate North Atlantic and Pacific stacks increases slightly with time, changing from 0.71‰ at 2.5–3 Ma to 0.88‰ at 0–0.5 Ma. The middle deep Atlantic stack is quite similar to the intermediate North Atlantic from 1.5 to 3 Ma but
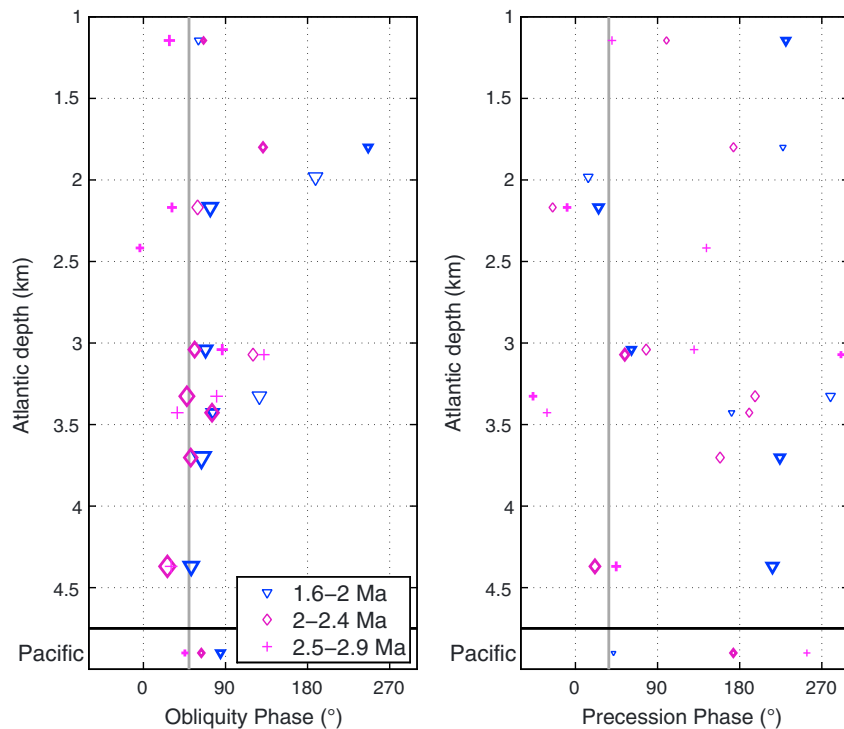
Figure 5. Obliquity and precession phase lags of Atlantic δ^{13}C as a function of depth for 1.6–3 Ma. Pacific δ^{13}C stack phases are shown at the bottom for comparison. Phases are plotted relative to ETP for 400 kyr windows centered at 1.8 Ma (blue triangles), 2.2 Ma (purple diamonds), and 2.7 Ma (pink crosses). Symbol sizes are proportional to the log of spectral density, and bold symbols indicate 80% coherence with ETP. Vertical gray lines show the mean phase of benthic δ^{18}O from 1.6 to 3 Ma.

displays consistently lower glacial δ^{13}C values beginning at 1.5 Ma. Glacial δ^{13}C gradients between the intermediate and middle deep Atlantic stacks may reflect the intrusion of δ^{13}C-depleted SCW into the middle deep Atlantic and, thus, glacial shoaling of NCW-SCW boundary. Glacial gradients between the intermediate and middle deep Atlantic increase again at ~0.9 Ma, with middle deep Atlantic δ^{13}C reaching values nearly as low as Pacific δ^{13}C. *Raymo et al.* [1997] interpreted this as evidence of greater glacial shoaling beginning at 0.9 Ma.

4.2. δ^{13}C Obliquity and Precession Responses

Figure 4 shows the obliquity and precession phase lags of all Atlantic δ^{13}C records as a function of depth for nonoverlapping 400 kyr windows from 0 to 1.6 Ma. Several patterns of response appear to hold true for individual Atlantic δ^{13}C records since 1.6 Ma. The obliquity and precession phase lags of cores above 2200 m tend be larger and more variable than deeper cores. The obliquity phases of Atlantic δ^{13}C records below 2350 m have a phase range of 6–117°, approximately centered around the phase of benthic δ^{18}O (58°). However, in the precession band nearly all Atlantic δ^{13}C records below 2350 m lag benthic δ^{18}O (75°). These differences as a function of depth are used as the criteria for defining the boundary between the intermediate and middle deep Atlantic stacks. However, due to the absence of long records from 2350 to 3000 m, the middle deep stack contains no cores above 3000 m. The phase distinction between middle deep and lower deep Atlantic records is less clear, but precession lags for 0–0.4 Ma appear to be slightly smaller on average below ~4050 m.

Figure 5 shows the obliquity and precession phases of individual δ^{13}C records before 1.6 Ma. The obliquity phases of δ^{13}C appear similar to those after 1.6 Ma, with phases below 2000 m clustered around the phase of benthic δ^{18}O. However, precession phases before 1.6 Ma are considerably different from those after 1.6 Ma. A large range of precession phases is observed at all depths, and it is difficult to discern any large-scale pattern. Precession power is weak at most sites, and only a few sites have statistically significant coherence.

The obliquity- and precession-band power and phase of the regional δ^{13}C stacks (Figure 6) are generally representative of their individual component records since 1.6 Ma. However, western Atlantic sites on the Ceara Rise have approximately twice as much precession power as other middle deep Atlantic sites (Figure S3).
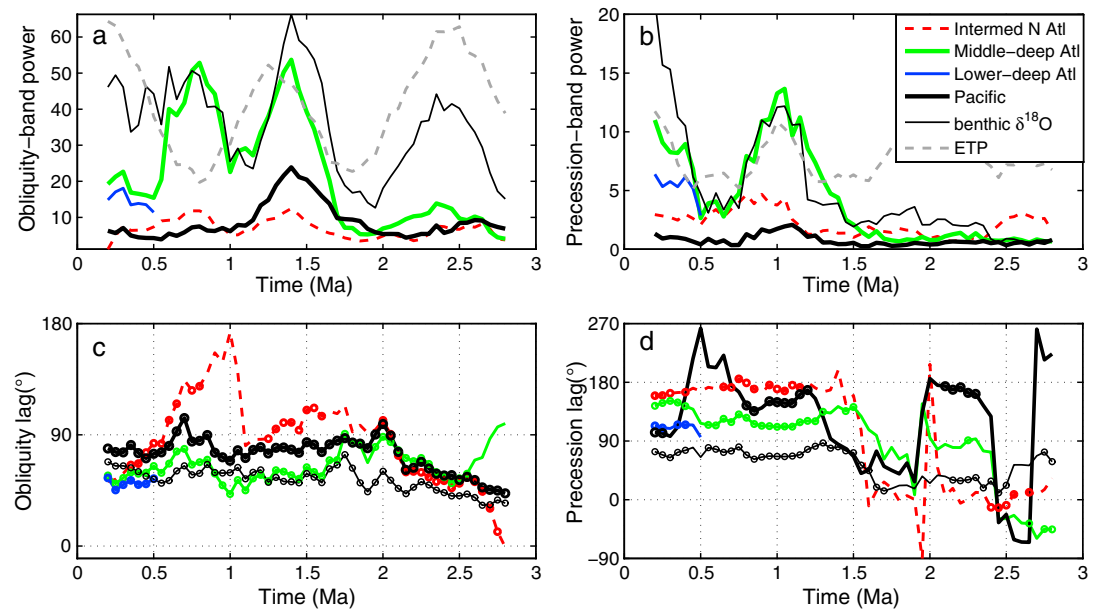
Figure 6. Orbital power and phase of regional δ^{13}C stacks. Plotted are spectral density in the (a) 41 kyr obliquity and (b) 23 kyr precession bands and (c and d) the corresponding phase lags relative to ETP from 400 kyr moving windows. Results are plotted for the benthic δ^{18}O stack (thin black), intermediate North Atlantic δ^{13}C (dashed red), middle deep Atlantic δ^{13}C (green), lower deep Atlantic δ^{13}C (blue), and Pacific δ^{13}C (thick black). Circles mark phases that are coherent with ETP at the 80% confidence level. The spectral power of ETP (dashed gray) is also shown, scaled vertically for better display.

Before 1.6 Ma the precession phases of individual middle deep Atlantic δ^{13}C records differ greatly from one another (Figures 5 and S3).

Since 1.5 Ma the middle deep Atlantic stack contains considerably more obliquity and precession power than the Pacific and intermediate North Atlantic stacks (Figures 6a and 6b). Because the orbital power in Pacific δ^{13}C is generally less than one fourth the power middle deep Atlantic δ^{13}C after 1.5 Ma, changes in mean ocean δ^{13}C are unlikely to have had much effect on middle deep Atlantic δ^{13}C orbital responses since that time. A modest peak in Pacific δ^{13}C obliquity power at 1.4 Ma suggests that possibly as much ∼40% of middle deep Atlantic obliquity power from 1.15 to 1.5 Ma could be related to mean δ^{13}C change. Similarly, the weak orbital power of intermediate North Atlantic δ^{13}C suggests that middle deep δ^{13}C variability is not likely caused by NCW δ^{13}C change, except perhaps during the weak precession response in middle deep Atlantic δ^{13}C from 0.5 to 0.75 Ma. Therefore, most middle deep Atlantic responses likely indicate shoaling of the NCW-SCW boundary and/or changes in the δ^{13}C value of SCW rather than changes in mean ocean δ^{13}C or NCW δ^{13}C.

Changes in the orbital power and phases of the regional δ^{13}C stacks through time may help constrain the forcing mechanisms for circulation changes. Middle deep Atlantic precession power peaks at 0–0.4 Ma and 1 Ma during maxima in precession forcing and benthic δ^{18}O power. Middle deep obliquity power peaks during a maximum in obliquity forcing at 1.4 Ma but also at 0.8 Ma during a minimum in obliquity forcing. The obliquity phases of all δ^{13}C stacks are in phase with or slightly lagging benthic δ^{18}O throughout most of the last 3 Ma (Figure 6c). Two exceptions occur in the intermediate North Atlantic, which has a larger obliquity lag from 0.7 to 1 Ma and leads δ^{18}O at 2.75 Ma. In the precession band (Figure 6d), the intermediate and middle deep Atlantic stacks have large and approximately constant lags relative to benthic δ^{18}O since 1.5 Ma, while the lower deep Atlantic stack has a smaller precession lag. The Pacific stack switches from a large lag before 0.8 Ma (where coherent) to a small lag at ∼0.3 Ma.

4.3. North Atlantic SST

The three records of SST at Site 607/U1313 show similar variations in obliquity phase and precession power since 3 Ma (Figure 7) but differ substantially with respect to obliquity power from 0.8 to 1.5 Ma and precession phase from 0 to 3 Ma. All three North Atlantic SST records have relatively weak obliquity power during the late Pleistocene, but they differ in the time of peak obliquity power. The two alkenone records show a peak in obliquity power at 1.4 Ma, coincident with peak obliquity power in benthic δ^{18}O and middle deep
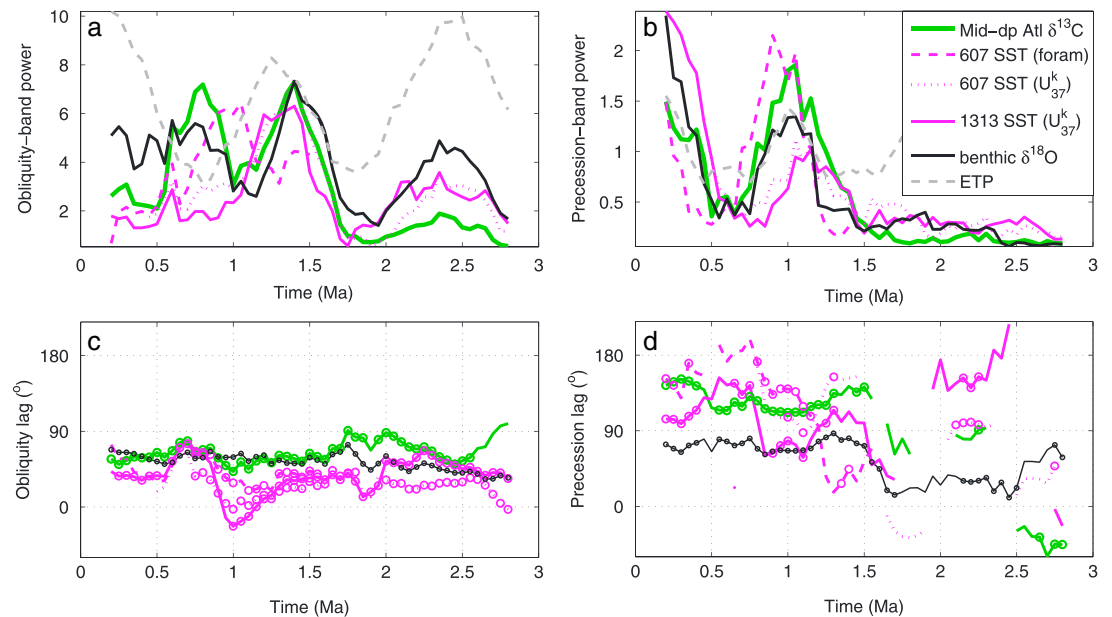
Figure 7. North Atlantic SST orbital power and phase. Axes are similar to Figure 6, showing (a) obliquity and (b) precession power and (c and d) phase lags relative to ETP with circles marking 80% coherence. Results are plotted for summer SST at Site 607 (dashed pink) [*Ruddiman et al.*, 1989], mean annual SST at Site 607 (dotted pink) [*Lawrence et al.*, 2010], mean annual SST at Site U1313 (solid pink) [*Naafs et al.*, 2012], middle deep Atlantic δ^{13}C (green), and benthic δ^{18}O (black). The orbital power of each proxy is scaled based on its average precession-band power from 0 to 1.0 Ma. For clarity, SST phase data are only shown for coherence values above 0.5.

Atlantic δ^{13}C, but the obliquity power peak in summer SST occurs at 1 Ma. The obliquity phase of all three SST records leads benthic δ^{18}O and middle deep Atlantic δ^{13}C throughout most of the last 1.6 Ma.

Changes in the precession power of all three SST records correlate reasonably well with ice volume, orbital forcing, and middle deep Atlantic δ^{13}C (Figure 7b). However, the three records show substantial differences in precession phase, especially before 1.2 Ma. For most of the last 1.2 Ma, the three SST records lag benthic δ^{18}O. Site 607 summer SST has the largest phase lag (often lagging middle deep Atlantic δ^{13}C), and Site U1313 SST has the smallest (usually leading δ^{13}C). However, from 0.6 to 0.8 Ma where the U1313 age model is best constrained, U1313 SST does lag δ^{13}C. A particularly small phase lag for summer SST at 1.3–1.5 Ma corresponds with an interval of weak precession power and large SST differences between the proxies (Figure S2).
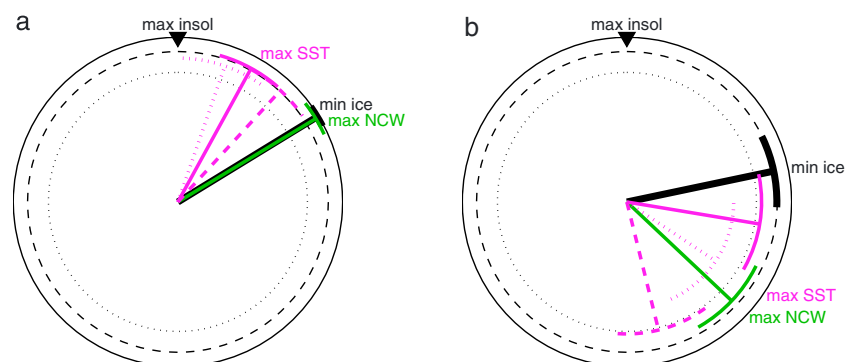
Figure 8. Zero to 1.5 Ma phase wheels for (a) obliquity and (b) precession. Vectors show the phases of interglacial-type responses in benthic δ^{18}O (black), middle deep Atlantic δ^{13}C (green), summer SST at Site 607 (dashed pink) [*Ruddiman et al.*, 1989], $U_{37}^{k'}$ SST at Site 607 (dotted pink) [*Lawrence et al.*, 2010], and $U_{37}^{k'}$ SST at Site U1313 (solid pink) [*Naafs et al.*, 2012]. Maximum NH summer insolation is marked by a black triangle at the top of each circle. Phase lags increase in the clockwise direction. Vector length represents coherency with ETP, and the associated arc denotes phase error at the 80% confidence level. Circles mark 100% (solid), 95% (dashed), and 80% (dotted) coherency.

Table 2. Obliquity and Precession Responses of Climate and Circulation Proxies From 0 to 1.5 Ma[a]

	41 kyr			23 kyr		
Proxy	Coherency	Phase (deg)	Phase (kyr)	Coherency	Phase (deg)	Phase (kyr)
$-1 \times$ benthic δ^{18}O	0.99	59 ± 4	6.7	0.91	78 ± 14	5.0
Middle deep Atl δ^{13}C	0.98	59 ± 7	6.7	0.88	133 ± 17	8.5
607 summer SST	0.92	43 ± 13	4.9	0.80	166 ± 22	10.6
607 $U_{37}^{k\prime}$ SST	0.87	19 ±v17	2.2	0.65	123 ± 33	7.9
U1313 $U_{37}^{k\prime}$ SST	0.93	29 ± 13	3.3	0.82	99 ± 21	6.4

[a]Phases are given for interglacial-type climate responses relative to ETP with 80% confidence intervals. Coherency with ETP is significant at 0.79 (80% confidence) and 0.91 (95% confidence).

4.4. Phase Comparisons 0–1.5 Ma

Phase wheels (Figure 8 and Table 2) summarize mean obliquity and precession phases from 0 to 1.5 Ma. Triangles at the top mark maximum NH summer insolation for both orbital bands, and phase lags increase clockwise. Lines indicate the phase of interglacial-type responses (i.e., minimum ice volume, maximum NCW, and maximum SST), and arcs show their 80% confidence intervals. Significantly different patterns of response are observed at these two orbital frequencies. In the obliquity band maximum North Atlantic SST slightly leads benthic δ^{18}O and middle deep Atlantic δ^{13}C, which both have a lag of 59° (6.7 kyr) relative to maximum NH summer insolation. However, middle deep Atlantic δ^{13}C and North Atlantic SST both lag benthic δ^{18}O in the precession band. The precession lag of middle deep Atlantic δ^{13}C relative to benthic δ^{18}O is 55° (3.5 kyr) and statistically significant, compared with no observed lag between δ^{13}C and δ^{18}O in the obliquity band. Although phase estimates for North Atlantic SST differ between the three proxy records, all three lead benthic δ^{18}O in the obliquity band but lag it in the precession band.

5. Discussion

5.1. Proxy Interpretations

In *Lisiecki et al.* [2008] the precession phase of summer SST at DSDP Site 607 was used as evidence that middle deep Atlantic $\Delta\delta^{13}$C reflects changes in NCW overturning rate from 0 to 0.4 Ma. In that study, North Atlantic SST and middle deep Atlantic $\Delta\delta^{13}$C both significantly lag benthic δ^{18}O in the precession band but are in phase with or leading δ^{18}O in the obliquity band. Because SST should respond rapidly to forcing, it is unlikely that large North Atlantic SST precession lags represent a delayed SST response to NH summer insolation or ice volume. Instead, it is more likely that North Atlantic SST phase is responding to changes in northward heat transport associated with circulation change as recorded by middle deep Atlantic $\Delta\delta^{13}$C. Similar relationships between ice volume, middle deep Atlantic δ^{13}C, and North Atlantic SST are observed in this study from 0 to 1.5 Ma using three North Atlantic SST proxy records.

In this study the obliquity phase relationship between North Atlantic SST and benthic δ^{18}O is clearer because all three SST proxies have similar obliquity phases which lead benthic δ^{18}O, demonstrating the expected rapid response to changes in insolation and possibly circulation or ice volume. (Because SST obliquity phase occurs between insolation and δ^{18}O/δ^{13}C, it could indicate a combined response to these forcings.) An additional difference from *Lisiecki et al.* [2008] is that middle deep Atlantic $\Delta\delta^{13}$C leads benthic δ^{18}O while this study finds that middle deep Atlantic δ^{13}C is in phase with δ^{18}O. The 49° phase difference for middle deep Atlantic δ^{13}C between the two studies is explained by a combination of several factors: a different collection of middle deep Atlantic sites, a different time window, and small differences between $\Delta\delta^{13}$C and δ^{13}C.

Agreement between the two studies is even stronger in the precession band. Both studies find that middle deep Atlantic δ^{13}C (or $\Delta\delta^{13}$C) and summer North Atlantic SST lag benthic δ^{18}O. Although the precession phase lags of the two alkenone SST proxies are not statistically significant relative to benthic δ^{18}O, the SST precession lags are all significantly larger than in the obliquity band, where SST leads benthic δ^{18}O. Differences between the precession phase estimates of the three SST records may result from age model uncertainty and differences in the seasonality and water depth sampled by the two proxies. (However, winter and summer SST estimates from *Ruddiman et al.* [1989] have nearly identical obliquity and precession phase lags.) Because age model uncertainty and intervals of weak orbital power could produce apparent changes in the phase of North Atlantic SST through time (Figure 7), the mean phase from 0 to 1.5 Ma is likely more reliable than shorter-term measurements.

Comparison of obliquity and precession phases for all three North Atlantic SST records demonstrates that some factor other than ice volume delays SST responses more in the precession band than the obliquity band. North Atlantic SST is strongly affected by changes in Atlantic overturning (NCW formation rates) during the last deglaciation [*McManus et al.*, 2004; *Shakun et al.*, 2012], and a similar relationship with orbital-band circulation changes would explain the obliquity and precession phases observed here. Specifically, North Atlantic SST obliquity and precession phases can both be explained if the phase of middle deep Atlantic δ^{13}C represents greater Atlantic overturning, such that greater overturning increases middle deep Atlantic δ^{13}C values and warms the North Atlantic (by increasing northward heat transport). Thus, although middle deep Atlantic δ^{13}C does not directly measure overturning rate or %NCW, the relatively large precession lags of both middle deep Atlantic δ^{13}C and North Atlantic SST strongly suggest that middle deep Atlantic δ^{13}C since 1.5 Ma is recording large-scale, climatically significant changes in NCW formation rate.

5.2. Circulation Changes at 1.5 Ma

Middle deep Atlantic δ^{13}C values closely match intermediate North Atlantic values throughout glacial cycles from 1.5 to 3 Ma. Because depleted δ^{13}C values are observed at deeper and more southerly sites (Figure S1), it appears that the NCW-SCW boundary rarely shoaled above 3500–4000 m before 1.5 Ma, in agreement with *Bickert et al.* [1997] and *McIntyre et al.* [1999]. Relatively weak orbital power and fewer δ^{13}C records make it difficult to characterize the orbital responses in end-member δ^{13}C or water mass boundaries before this time (Figure 5).

A change in Atlantic circulation at 1.5–1.6 Ma is indicated by the appearance of glacial δ^{13}C gradients between the intermediate and middle deep Atlantic stacks, increases in the obliquity and precession power of middle deep Atlantic δ^{13}C relative to other regions, and a rapid transition in the precession phase of Atlantic δ^{13}C records spanning a wide range of depths. The exact timing of this transition is difficult to identify, but it seems to occur first (~1.6 Ma) at sites below 3300 m (ODP 927, 929, and 1090) and later (~1.5 Ma) at shallower ODP Sites 925 and 981 (e.g., Figure S3). Benthic δ^{18}O also experiences a shift in precession phase (but not obliquity phase) at ~1.5 Ma, potentially suggesting a climate-wide change in precession responses. Although this phase shift could be an artifact of the LR04 age model, it is unlikely that an age model error would shift the stack's precession phase while its obliquity phase remained relatively constant [*Lisiecki and Raymo*, 2005].

The obliquity and precession power of the middle deep Atlantic and Pacific δ^{13}C stacks also begin to covary with δ^{18}O power at ~1.6 Ma (Figure 6). Increases in middle deep Atlantic obliquity power at 1.65 Ma and precession power at ~1.5 Ma may indicate greater glacial shoaling of NCW caused by increases in both orbital forcing and ice volume. Similar changes at ODP Site 1090 have been interpreted as a decrease in glacial SCW ventilation [*Venz and Hodell*, 2002; *Hodell and Venz-Curtis*, 2006]. Increases in the orbital power of Pacific δ^{13}C are smaller but similar in timing to those of other proxies and could be caused by a changes in SCW δ^{13}C, the relative flux of NCW and SCW to the Pacific, and/or mean ocean δ^{13}C change.

Hodell and Venz-Curtis [2006] also identify ~1.55 Ma as an important climate transition because it marks the time when glacial δ^{13}C values of the deep South Atlantic (ODP Site 1090) became more negative than glacial Pacific δ^{13}C. They attribute this change to reduced ventilation of deep SCW caused by surface changes in Antarctic source areas (e.g., increased sea ice and enhanced surface stratification) and suggest that a positive feedback between deep water ventilation and atmospheric pCO$_2$ may have caused cooling at this time. Direct measurements of pCO$_2$ are not available before 0.8 Ma, and indirect proxies have large error bars and relatively low resolution [e.g., *Hönisch et al.*, 2009; *Tripati et al.*, 2009]. However, several SST records show a cooling trend beginning at ~1.5 Ma [*Herbert et al.*, 2010; *Marlow et al.*, 2000; *Lawrence et al.*, 2010; *Naafs et al.*, 2012]. The increased variability in the middle deep Atlantic and deep Pacific δ^{13}C observed at ~1.5 Ma in this study further suggests that these glacial circulation changes may have altered the carbon storage of most of the deep ocean. Therefore, orbital-scale pCO$_2$ changes may have greatly increased in amplitude at 1.5 Ma, perhaps more dramatically than during the MPT [*Lisiecki*, 2010b].

No large changes in the obliquity or precession phases of middle deep Atlantic δ^{13}C are observed since 1.5 Ma. Age model uncertainty for Sites 607 and U1313 and differences between proxies prevents identification of any transitions in the phase lags of North Atlantic SST. However, North Atlantic SST does show a strong cooling trend from 1.6 to 0.8 Ma (Figure S2) [*Lawrence et al.*, 2010; *Naafs et al.*, 2012].

5.3. Mid-Pleistocene Transition

An increase in the gradient between intermediate and middle deep Atlantic $\delta^{13}C$ during glaciations beginning at 0.9 Ma likely indicates a circulation response (probably greater NCW shoaling and/or less SCW ventilation) to the increased size of NH ice sheets [e.g., *Raymo et al.*, 1997; *Clark et al.*, 2006; *Bintanja and van de Wal*, 2008]. *Lawrence et al.* [2010] suggest that SCW influence in the middle deep North Atlantic increased beginning at 1 Ma. Although larger deglacial meltwater fluxes since 0.9 Ma could conceivably have caused a shift in the obliquity and precession phases of NCW formation, there is no evidence for such a change. Other studies more focused on 100 kyr cyclicity or the relative timing of events during deglaciation would be better suited to characterize circulation responses to the rapid deglaciation of larger ice sheets.

No phase shifts are observed in middle deep Atlantic $\delta^{13}C$ at the MPT, but two other changes are observed in Atlantic obliquity responses (Figure 6). First, the phase lag of intermediate North Atlantic $\delta^{13}C$ increased at ~1 Ma and then steadily declined from 0.7 to 0.4 Ma. Second, the obliquity power of middle deep Atlantic $\delta^{13}C$ decreased by 50% at 0.6 Ma despite relatively constant 41 kyr power in benthic $\delta^{18}O$. Because this decrease was concurrent with dramatic increases in the 100 kyr power of benthic $\delta^{18}O$ and middle deep Atlantic $\delta^{13}C$ (Figure S4), it may indicate that the effects of 100 kyr glacial variability restricted obliquity-driven overturning changes. The only $\delta^{13}C$ precession response which might be associated with the MPT is a short-term increase in the precession lag of Pacific $\delta^{13}C$ (Figure 6d), but this is likely an artifact of measurement uncertainty due to the extremely weak precession power at this time.

5.4. Mid-Brunhes Event

The Mid-Brunhes Event (MBE) at 0.4 Ma is associated with several changes in $\delta^{13}C$ precession responses. At this time the precession power of middle deep Atlantic $\delta^{13}C$ doubles, most likely as the result of increased precession power in orbital forcing and/or ice volume (Figure 7b), and the precession phase of middle deep Atlantic $\delta^{13}C$ increases from 120° to 150°. Additionally, Pacific $\delta^{13}C$ becomes coherent with precession again, and its phase lag decreases from ~150° (at 0.8–1.2 Ma) to 100° (Figure 6). These changes in the precession response of Pacific $\delta^{13}C$ could indicate a tighter coupling between ocean CO_2 storage and ice volume since ~0.4 Ma [*Lisiecki*, 2010b] and may help explain the increased amplitude of pCO_2 observed since the MBE [*Siegenthaler et al.*, 2005].

6. Conclusions

Thirty-nine Atlantic and seven Pacific $\delta^{13}C$ records were analyzed to study the obliquity and precession responses of deep water circulation from 0 to 3 Ma. Middle deep Atlantic $\delta^{13}C$ responses (2300–4010 m) are indicative of NCW shoaling and/or SCW ventilation changes and likely also correspond to changes in overturning rate of since at least 1.5 Ma (based on comparison with the precession phase of North Atlantic SST). Spectral analysis of these records indicates that the obliquity and precession responses of Atlantic circulation changed at ~1.5 Ma in connection with the appearance of glacial $\delta^{13}C$ gradients between intermediate and middle deep Atlantic $\delta^{13}C$. Since that time the obliquity and precession power of middle deep Atlantic $\delta^{13}C$ greatly exceeds that of intermediate North Atlantic and Pacific $\delta^{13}C$. Additionally, since 1.5 Ma nearly all middle deep Atlantic $\delta^{13}C$ records are approximately in phase with benthic $\delta^{18}O$ in the obliquity band but lag $\delta^{18}O$ in the precession band. The MPT had little effect on these phases but likely contributed to a ~50% decrease in the obliquity power of middle deep Atlantic $\delta^{13}C$ at 0.6 Ma.

References

Abe-Ouchi, A., F. Sato, K. Kawamura, M. E. Raymo, J. Okuno, K. Takahashi, and H. Blatter (2013), Insolation-driven 100,000-year glacial cycles and hysteresis of ice-sheet volume, *Nature*, *500*, 190–193.

Alonso-Garcia, M., F. J. Sierro, M. Kucera, J. A. Flores, I. Cacho, and N. Andersen (2011), Ocean circulation, ice sheet growth and interhemispheric coupling of millennial climate variability during the mid-Pleistocene (ca 800–400 ka), *Quat. Sci. Rev.*, *30*, 3234–3247.

Bartoli, G., M. Sarnthein, and M. Weinelt (2006), Late Pliocene millennial-scale climate variability in the northern North Atlantic prior to and after the onset of Northern Hemisphere glaciation, *Paleoceanography*, *21*, PA4205, doi:10.1029/2005PA001185.

Belanger, P. E., W. B. Curry, and R. K. Matthews (1981), Core top evaluation of benthic foraminiferal isotopic ratios for paleoceanographical interpretations, *Palaeogeogr. Palaeoclimatol. Palaeoecol.*, *33*, 205–221.

Bickert, T., and G. Wefer (1996), Late Quaternary deep water circulation in the South Atlantic: Reconstruction from carbonate dissolution and benthic stable isotopes, in *The South Atlantic: Present and Past Circulation*, edited by G. Wefer et al., pp. 599–620, Springer, New York.

Bickert, T., W. B. Curry, and G. Wefer (1997), Late Pliocene to Holocene (2.6–0 Ma) western equatorial Atlantic deep-water circulation: Inferences from benthic stable isotopes, in *Proceedings of the Ocean Drilling Program, Sci. Results*, vol. 154, edited by N. J. Shackleton et al., pp. 239–254, Ocean Drilling Program, College Station, Tex.

Bintanja, R., and R. S. W. van de Wal (2008), North American ice-sheet dynamics and the onset of 100,000-year glacial cycles, *Nature*, *454*, 869–872.

Cheng, X., J. Tian, and P. Wang (2004), Data report: Stable isotopes from Site 1143, in *Proceedings of the Ocean Drilling Program, Sci. Results,* vol. 184, edited by W. L. Prell et al., Ocean Drilling Program, College Station, Tex., doi:10.2973/odp.proc.sr.184.221.2004.

Clark, P. U., D. Archer, D. Pollard, J. D. Blum, J. A. Rial, V. Brovkin, A. C. Mix, N. G. Pisias, and M. Roy (2006), The middle Pleistocene transition: Characteristics, mechanisms, and implications for long-term changes in atmospheric pCO_2, *Quat. Sci. Rev.*, *25*, 3150–3184.

Curry, W. B. (1996), Late Quaternary deep circulation in the western equatorial Atlantic, in *The South Atlantic: Present and Past Circulation*, edited by G. Wefer et al., pp. 599–620, Springer, New York.

Curry, W. B., J.-C. Duplessy, L. Labeyrie, and N. J. Shackleton (1988), Changes in the distribution of $\delta^{13}C$ of deep water ΣCO_2 between the last glaciation and the Holocene, *Paleoceanography*, *3*, 317–341, doi:10.1029/PA003i003p00317.

Curry, W. B., and D. W. Oppo (1997), Synchronous, high-frequency oscillations in tropical sea surface temperatures and North Atlantic Deep Water production during the last glacial cycle, *Paleoceanography*, *12*, 1–14.

Curry, W. B., T. M. Marchitto, J. F. McManus, D. W. Oppo, and K. L. Laarkamp (1999), Millennial-scale changes in ventilation of the thermocline, intermediate, and deep waters of the glacial North Atlantic, in *Mechanisms of Global Climate Change at Millennial Time Scales, Geophys. Monogr. Ser.,* vol. 112, edited by P. U. Clark, R. S. Webb, and L. D. Keigwin, pp. 59–76, AGU, Washington, D. C.

Curry, W. B., and D. W. Oppo (2005), Glacial water mass geometry and the distribution of $\delta^{13}C$ of ΣCO_2 in the western Atlantic Ocean, *Paleoceanography*, *20*, PA1017, doi:10.1029/2004PA001021.

deMenocal, P. B., D. W. Oppo, R. G. Fairbanks, and W. L. Prell (1992), Pleistocene $\delta^{13}C$ variability of North Atlantic intermediate water, *Paleoceanography*, *7*, 229–250.

Duplessy, J. C., N. J. Shackleton, R. G. Fairbanks, L. Labeyrie, D. Oppo, and N. Kallel (1988), Deepwater source variations during the last climatic cycle and their impact on the global deepwater circulation, *Paleoceanography*, *3*, 343–360.

Flower, B. P., D. W. Oppo, J. F. McManus, K. A. Venz, D. A. Hodell, and J. L. Cullen (2000), North Atlantic intermediate to deep water circulation and chemical stratification during the past 1 Myr, *Paleoceanography*, *15*, 388–403.

Gebbie, G. (2014), How much did Glacial North Atlantic Water shoal?, *Paleoceanography*, doi:10.1002/2013PA002557.

Graham, D. W., B. H. Corliss, M. L. Bender, and L. D. Keigwin (1981), Carbon and oxygen isotopic disequilibria of recent deep-sea benthic foraminifera, *Mar. Micropaleontol.*, *6*, 483–479.

Hale, W., and U. Pflaumann (1999), Sea-surface temperature estimations using a modern analog technique with foraminiferal assemblages from western Atlantic Quaternary sediments, in *Use of Proxies in Paleoceanography– Examples From the South Atlantic*, edited by G. Fischer and G. Wefer, pp. 69–90, Springer, New York.

Harris, S. E. (2002), Data report: Late Pliocene-Pleistocene carbon and oxygen stable isotopes from benthic foraminifers at Ocean Drilling Program Site 1123 in the southwest Pacific, in *Proceedings of the Ocean Drilling Program, Sci. Results*, vol. 181, edited by C. Richter, pp. 1–10, Ocean Drilling Program, College Station, Tex., doi:10.2973/odp.proc.sr.181.203.2002.

Herbert, T. D., L. Cleaveland Peterson, K. T. Lawrence, and Z. Liu (2010), Tropical ocean temperatures over the past 3.5 million years, *Science*, *328*, 1530–1534.

Hesse, T., M. Butzin, T. Bickert, and G. Lohmann (2011), A model-data comparison of $\delta^{13}C$ in the glacial Atlantic Ocean, *Paleoceanography*, *26*, PA3220, doi:10.1029/2010PA002085.

Hodell, D., C. Charles, and U. Ninnemann (2000), Comparison of interglacial stages in the South Atlantic sector of the southern ocean for the past 450 kyr: Implications for Marine Isotope Stage (MIS) 11, *Global Planet. Change*, *24*, 7–26.

Hodell, D. A., C. D. Charles, and F. J. Sierro (2001), Late Pleistocene evolution of the ocean's carbonate system, *Earth Planet. Sci. Lett.*, *192*, 109–124.

Hodell, D. A., C. D. Charles, J. H. Curtis, P. G. Mortyn, U. S. Ninnemann, and K. A. Venz (2003), Data report: Oxygen isotope stratigraphy of ODP Leg 177 Sites 1088, 1089, 1090, 1093, and 1094, in *Proceedings of the Ocean Drilling Program, Sci. Results,* vol. 177, edited by R. Gersonde, D. A. Hodell, and P. Blum, pp. 1–26, Ocean Drilling Program, College Station, Tex.

Hodell, D. A., and K. A. Venz-Curtis (2006), Late Neogene history of deepwater ventilation in the Southern Ocean, *Geochem. Geophys. Geosyst.*, *7*, Q09001, doi:10.1029/2005GC001211.

Hodell, D. A., J. E. T. Channell, J. H. Curtis, O. E. Romero, and U. Röhl (2008), Onset of "Hudson Strait" Heinrich events in the eastern North Atlantic at the end of the middle Pleistocene transition (∼640 ka)?, *Paleoceanography*, *23*, PA4218, doi:10.1029/2008PA001591.

Hodell, D., S. Crowhurst, L. Skinner, P. C. Tzedakis, V. Margari, J. E. T. Channell, G. Kamenov, S. Maclachlan, and G. Rothwell (2013), Response of Iberian Margin sediments to orbital and suborbital forcing over the past 420 ka, *Paleoceanography*, *28*, 185–199, doi:10.1002/palo.20017.

Hönisch, B., N. G. Hemming, D. Archer, M. Siddall, and J. F. McManus (2009), Atmospheric carbon dioxide concentration across the mid-Pleistocene transition, *Science*, *324*, 1551–1553.

Imbrie, J., et al. (1992), On the structure and origin of major glaciation cycles. 1. Linear responses to Milankovitch forcing, *Paleoceanography*, *7*, 701–738.

Kroopnick, P. M. (1985), The distribution of $\delta^{13}C$ of ΣCO_2 in the world oceans, *Deep Sea Res. Part A*, *32*, 57–84.

Lawrence, K. T., S. Sosdian, H. E. White, and Y. Rosenthal (2010), North Atlantic climate evolution through the Plio-Pleistocene climate transitions, *Earth Planet. Sci. Lett.*, *300*, 329–342.

Lisiecki, L. E. (2010a), Links between eccentricity forcing and the 100,000-year glacial cycle, *Nat. Geosci.*, *3*, 349–352.

Lisiecki, L. E. (2010b), A benthic $\delta^{13}C$-based proxy for atmospheric pCO_2 over the last 1.5 Myr, *Geophys. Res. Lett.*, *37*, L21708, doi:10.1029/2010GL045109.

Lisiecki, L. E., and P. A. Lisiecki (2002), Application of dynamic programming to the correlation of paleoclimate records, *Paleoceanography*, *17*(4), 1049, doi:10.1029/2001PA000733.

Lisiecki, L. E., and M. E. Raymo (2005), A Pliocene-Pleistocene stack of 57 globally distributed benthic $\delta^{18}O$ records, *Paleoceanography*, *20*, PA1003, doi:10.1029/2004PA001071.

Lisiecki, L. E., and M. E. Raymo (2009), Diachronous benthic $\delta^{18}O$ responses during late Pleistocene terminations, *Paleoceanography*, *24*, PA3210, doi:10.1029/2009PA001732.

Lisiecki, L. E., M. E. Raymo, and W. B. Curry (2008), Atlantic overturning responses to Late Pleistocene climate forcings, *Nature*, *456*, 85–88.

Mackensen, A., H.-W. Hubberten, T. Bickert, G. Fischer, and D. K. Fütterer (1993), $\delta^{13}C$ in benthic foraminiferal tests of Fontbotia wuellerstorfi (Schwager) relative to $\delta^{13}C$ of dissolved inorganic carbon in Southern Ocean deep water: Implications for glacial ocean circulation models, *Paleoceanography*, *8*, 587–610.

Marlow, J. R., C. B. Lange, G. Wefer, and A. Rosell-Mele (2000), Upwelling intensification as part of the Pliocene-Pleistocene climate transition, *Science*, *290*, 2288–2291.

McIntyre, K., A. C. Ravelo, and M. L. Delaney (1999), North Atlantic Intermediate Waters in the late Pliocene to early Pleistocene, *Paleoceanography*, *14*, 324–335.

McManus, J. F., D. W. Oppo, and J. L. Cullen (1999), A 0.5-million-year record of millennial-scale climate variability in the North Atlantic, *Science*, *283*, 971–975.

McManus, J. F., R. Francois, J.-M. Gherardi, L. D. Keigwin, and S. Brown-Leger (2004), Collapse and rapid resumption of Atlantic meridional circulation linked to deglacial climate changes, *Nature*, *428*, 834–837.

Miller, M. D., J. F. Adkins, D. Menemenlis, and M. P. Schodlok (2012), The role of ocean cooling in setting glacial southern source bottom water salinity, *Paleoceanography*, *27*, PA3207, doi:10.1029/2012PA002297.

Mix, A. C., J. Le, and N. J. Shackleton (1995a), Benthic foraminiferal stable isotope stratigraphy from Site 846: 0–1.8 Ma, in *Proceedings of the Ocean Drilling Program, Sci. Results,* vol. 138, edited by N. G. Pisias et al., pp. 839–854, Ocean Drilling Program, College Station, Tex.

Mix, A. C., N. G. Pisias, W. Rugh, J. Wilson, A. Morey, and T. K. Hagelberg (1995b), Benthic foraminifer stable isotope record from Site 849 (0–5 Ma): Local and global climate changes, in *Proceedings of the Ocean Drilling Program, Sci. Results,* vol. 138, edited by N. G. Pisias et al., pp. 371–412, Ocean Drilling Program, College Station, Tex.

Naafs, B. D. A., J. Hefter, P. Ferretti, R. Stein, and G. H. Haug (2011), Sea surface temperatures did not control the first occurrence of Hudson Strait Heinrich events during MIS 16, *Paleoceanography*, *26*, PA4201, doi:10.1029/2011PA002135.

Naafs, B. D. A., J. Hefter, G. Acton, G. H. Haug, A. Martinez-Garcia, R. Pancost, and R. Stein (2012), Strengthening of North American dust sources during the late Pliocene (2.7 Ma), *Earth Planet. Sci. Lett.*, *317–318*, 8–19.

Oppo, D. W., and R. G. Fairbanks (1987), Variability in the deep and intermediate water circulation of the Atlantic Ocean during the past 25,000 years: Northern Hemisphere modulation, *Earth Planet. Sci. Lett.*, *86*, 1–15.

Oppo, D. W., R. G. Fairbanks, A. L. Gordon, and N. J. Shackleton (1990), Late Pleistocene Southern Ocean ^{13}C variability, *Paleoceanography*, *5*, 43–54.

Oppo, D. W., J. F. McManus, and J. L. Cullen (1998), Abrupt climate events 500,000 to 340,000 years ago: Evidence from subpolar North Atlantic sediments, *Science*, *279*, 1335–1338.

Piotrowski, A. M., S. L. Goldstein, S. R. Hemming, and R. G. Fairbanks (2005), Temporal relationships of carbon cycling and ocean circulation at glacial boundaries, *Science*, *307*, 1933–1938.

Rau, A., J. Roger, J. Lutjeharms, J. Giraudeau, J. Lee-Thorp, M.-T. Chen, and C. Waelbroeck (2002), A 450-kyr record of hydrological conditions on the western Agulhas Bank Slope, south of Africa, *Mar. Geol.*, *180*, 183–201, doi:10.1016/S0025-3227(01)00213-4.

Raymo, M. E., W. F. Ruddiman, J. Backman, B. M. Clement, and D. G. Martinson (1989), Late Pliocene variation in Northern Hemisphere ice sheets and North Atlantic deep circulation, *Paleoceanography*, *4*, 413–446.

Raymo, M. E., D. W. Oppo, and W. Curry (1997), The mid-Pleistocene climate transition: A deep sea carbon isotope perspective, *Paleoceanography*, *12*, 46–559.

Raymo, M. E., K. Ganley, S. Carter, D. W. Oppo, and J. McManus (1998), Millennial-scale climate instability during the early Pleistocene epoch, *Nature*, *392*, 699–702.

Raymo, M. E., D. W. Oppo, B. P. Flower, D. A. Hodell, J. F. McManus, K. A. Venz, K. F. Kleiven, and K. McIntyre (2004), Stability of North Atlantic water masses in face of pronounced climate variability during the Pleistocene, *Paleoceanography*, *19*, PA2008, doi:10.1029/2003PA000921.

Rial, J. A., J. Oh, and E. Reischmann (2013), Synchronization of the climate system to eccentricity forcing and the 100,000-year problem, *Nat. Geosci.*, *6*, 289–293.

Ruddiman, W. F., M. E. Raymo, D. G. Martinson, B. M. Clement, and J. Backman (1989), Pleistocene evolution: Northern hemisphere ice sheets and North Atlantic Ocean, *Paleoceanography*, *4*, 353–412.

Sarnthein, M., H. Erlenkeuser, R. von Grafenstein, and C. Schröder (1984), Stable isotope stratigraphy for the last 750,000 years. Meteor core 13519 from the eastern equatorial Atlantic, *Meteor Forschungsergebnisse, Deutsche Forschungsgemeinschaft, Reihe C Geol. Geophys., Gebrüder Bornträger, Berlin, Stuttgart*, *C38*, 9–24.

Sarnthein, M., K. Winn, S. J. A. Jung, J.-C. Duplessy, L. Labeyrie, H. Erlenkeuser, and G. Ganssen (1994), Changes in east Atlantic deepwater circulation over the last 30,000 years: Eight time slice reconstructions, *Paleoceanography*, *9*, 209–267.

Shackleton, N. J., and M. A. Hall (1984), Oxygen and carbon isotope stratigraphy of DSDP Hole 552A: Plio-Pleistocene glacial history, *Initial Rep. Deep Sea Drill. Project*, *81*, 599–609.

Shackleton, N. J., A. Berger, and W. R. Peltier (1990), An alternative astronomical calibration of the lower Pleistocene timescale based on ODP Site 677, *Trans. R. Soc. Edinburgh Earth Sci.*, *81*, 251–261.

Shakun, J. D., P. U. clark, F. He, S. A. Marcott, A. C. Mix, Z. Liu, B. Otto-Bleisner, A. Schmittner, and E. Bard (2012), Global warming preceded by increasing carbon dioxide concentrations during the last deglaciation, *Nature*, *484*, 49–54.

Shin, S.-I., Z. Liu, B. L. Otto-Bliesner, J. E. Kutzbach, and S. J. Vavrus (2003), Southern Ocean sea-ice control of the glacial North Atlantic thermohaline circulation, *Geophys. Res. Lett.*, *30*(2), 1096, doi:10.1029/2002GL015513.

Siegenthaler, U., et al. (2005), Stable carbon cycle-climate relationship during the late Pleistocene, *Science*, *310*, 1313–1317.

Sigman, D. M., M. P. Hain, and G. H. Haug (2010), The polar ocean and glacial cycles in atmospheric CO_2 concentration, *Nature*, *466*, 47–55.

Skinner, L. C., and N. J. Shackleton (2005), An Atlantic lead over Pacific deep-water change across Termination I: Implications for the application of the marine isotope stage stratigraphy, *Quat. Sci. Rev.*, *24*, 571–580.

Sosdian, S., and Y. Rosenthal (2009), Deep-sea temperature and ice volume changes across the Pliocene-Pleistocene climate transition, *Science*, *325*, 306–310.

Tagliabue, A., L. Bopp, D. M. Roche, N. Bouttes, J. C. Dutay, R. Alkama, M. Kageyama, E. Michel, and D. Paillard (2009), Quantifying the roles of ocean circulation and biogeochemistry in governing ocean carbon-13 and atmospheric carbon dioxide at the last glacial maximum, *Clim. Past*, *5*, 695–706.

Tessin, A. C., and D. C. Lund (2013), Isotopically depleted carbon in the mid-depth South Atlantic during the last deglaciation, *Paleoceanography*, *28*, 296–306, doi:10.1002/palo.20026.

Tiedemann, R., M. Sarnthein, and N. J. Shackleton (1994), Astronomic timescale for the Pliocene Atlantic δ^{18}O and dust flux records of Ocean Drilling Program Site 659, *Paleoceanography*, *9*, 619–638.

Tripati, A. R., C. D. Roberts, and R. A. Eagle (2009), Coupling of CO_2 and ice sheet stability over major climate transitions of the last 20 million years, *Science*, *326*, 1394–1397.

Venti, N. L., and K. Billups (2012), Stable-isotope stratigraphy of the Pliocene-Pleistocene climate transition in the northwestern subtropical Pacific, *Palaeogeogr. Palaeoclimatol. Palaeoecol.*, *326–328*, 54–66.

Venz, K. A., D. A. Hodell, C. Stanton, and D. A. Warnke (1999), A 1.0 Myr record of Glacial North Atlantic Intermediate Water variability from ODP site 982 in the northeast Atlantic, *Paleoceanography*, *14*, 42–52.

Venz, K. A., and D. A. Hodell (2002), New evidence for changes in Plio-Pleistocene deep water circulation from Southern Ocean ODP Leg 177 Site 1090, *Palaeogeogr. Palaeoclimatol. Palaeoecol.*, *182*, 197–220.

Weber, S., et al. (2007), The modern and glacial overturning circulation in the Atlantic ocean in PMIP coupled model simulations, *Clim. Past*, *3*, 51–64.